

# Comparison of $H_{c2}(T, \theta)$ in $\text{Mg}_{1-x}\text{Al}_x\text{B}_2$ single crystals with the dirty-limit two-gap theory

Heon-Jung Kim<sup>1</sup>, Hyun-Sook Lee<sup>1</sup>, Byeongwon Kang<sup>1,†</sup>, Woon-Ha  
Yim<sup>1</sup>, Younghun Jo<sup>2</sup>, Myung-Hwa Jung<sup>2</sup>, and Sung-Ik Lee<sup>1,2</sup>

<sup>1</sup>*National Creative Research Initiative Center for  
Superconductivity and Department of Physics,  
Pohang University of Science and Technology,  
Pohang 790-784, Republic of Korea and*

<sup>2</sup>*Quantum Materials Research Laboratory,  
Korea Basic Science Institute, Daejeon 305-333, Republic of Korea*

(Dated: November 11, 2018)

## Abstract

We studied the temperature and the angular dependences of the upper critical field ( $H_{c2}(T, \theta)$ ) of  $\text{Mg}_{1-x}\text{Al}_x\text{B}_2$  single crystals ( $x = 0.12$  and  $0.21$ ) and compared with the dirty-limit two-gap theory. We found that  $H_{c2}(T, \theta)$ 's were well described in a unified way by this theory. The obtained values of the parameters indicated that as the Al concentration was increased, anisotropic impurity scattering increased, making the  $\sigma$  bands less anisotropic. Accordingly, the temperature dependence of the anisotropy ratio of  $H_{c2}$  ( $\gamma_H$ ) systematically decreased, and for  $x = 0.21$ ,  $\gamma_H$  was nearly constant. Our results imply that  $\text{Mg}_{1-x}\text{Al}_x\text{B}_2$  single crystals are in dirty-limit and that two-gap nature survives until  $x = 0.21$ .

PACS numbers: 74.70.Ad, 74.62.Dh, 74.62.Bf

It is now well established that MgB<sub>2</sub> is a two-gap superconductor with two distinct energy gaps: a large gap originating from two-dimensional  $\sigma$  bands and a small gap originating from three-dimensional  $\pi$  bands [1, 2, 3]. One of the main consequences of the two-gap nature is the strong temperature dependence of the  $H_{c2}(T)$  anisotropy,  $\gamma_H \equiv H_{c2}^{ab}/H_{c2}^c$  [4], which is not expected based on the single-gap Ginzburg-Landau theory. Theoretical calculations show that the strong temperature dependence of  $\gamma_H$  arises from the fact that the anisotropic  $\sigma$  bands dominate  $\gamma_H$  at low temperatures while the  $\pi$  bands gradually become important at temperatures near  $T_c$  [5, 6, 7]. The above anomalous behavior of  $\gamma(T)$  for MgB<sub>2</sub> single crystals was confirmed by using magnetization measurements [8, 9].

When impurity scattering is increased, the above-mentioned behaviors of  $H_{c2}$  are modified. Gurevich [6], and Golubov and Koshelev [7] formulated the dirty-limit two-gap theory for  $H_{c2}$  by using the quasiclassical Usadel equations. According to this theory, the shape of the  $H_{c2}(T)$  curve essentially depends on the diffusivities of the  $\sigma$  and the  $\pi$  bands. For  $T \approx T_c$ ,  $H_{c2}(T)$  is determined by a maximum diffusivity (cleaner bands) between  $D_\sigma$  and  $D_\pi$  while  $H_{c2}(0)$  is controlled by a minimum diffusivity (dirtier bands). When the  $\sigma$  bands are dirtier, an upward curvature should appear near  $T_c$ , and  $\gamma_H$  should decrease with temperature. In contrast, when the  $\pi$  bands are dirtier, a huge increase in  $H_{c2}(T)$  should appear at low temperatures without an upward curvature near  $T_c$ , and  $\gamma_H$  should increase with temperature.

Impurity scattering also changes  $H_{c2}(\theta)$ .  $H_{c2}(\theta)$  was predicted to deviate from the angular dependence of the anisotropic one-gap Ginzburg-Landau (GL) theory, especially near the middle-angle region. This deviation should be most pronounced at  $T/T_c \approx 0.95$  when the parameters supplied by band-structure calculations are used [7, 10]. Even though these predictions were quantitatively compared with  $H_{c2}(\theta)$  for MgB<sub>2</sub> single crystals and reasonable consistency was observed [10], the problem of whether the dirty-limit theory could be applied to clean MgB<sub>2</sub> single crystals still remained. In this sense, the dirty-limit theory has not yet been verified unambiguously for single crystals in the dirty limit, especially for the orientational dependence of  $H_{c2}$ .

In this paper, we report the effect of Al doping, as deduced from resistance measurements at various angles  $\theta$  between  $H$  and the  $c$ -axis, on  $H_{c2}(T, \theta)$  of Al-doped MgB<sub>2</sub> single crystals. This directional study of the resistance was possible due to success in growing flat and regular-shaped Mg<sub>1-x</sub>Al<sub>x</sub>B<sub>2</sub> single crystals with values of  $x$  up to 0.21 and with  $T_c = 25.5$  K.

We found that two-gap superconductivity in MgB<sub>2</sub> was drastically affected by the Al doping and that key features predicted by the dirty-limit two-gap theory were observed. Our main observations are the following: (1) As the Al concentration increases, the residual resistivity ( $\rho_0$ ) greatly increases, implying that Al substitution enhances impurity scattering and that the Al-doped samples are in the dirty-region. (2)  $H_{c2}(T)$  can be consistently explained within the dirty-limit two-gap theory up to  $x = 0.21$ , even though  $H_{c2}(0)$  decreases with Al concentration. (3) The  $\gamma_H(T)$  systematically decreases and for  $x = 0.21$ ,  $\gamma_H$  is virtually temperature-independent. (4) The  $H_{c2}(\theta)$  for  $x = 0.12$  showed a clear deviation from the behavior predicted by the anisotropic GL theory, which is a strong indication of the two-gap nature in MgB<sub>2</sub>. However, for  $x = 0.21$ , this deviation became very small. The values of the obtained parameters suggest that impurity scattering is enhanced in the  $\pi$  bands, especially along the  $c$  direction and that the anisotropy of the  $\sigma$  bands is significantly reduced.

Mg<sub>1-x</sub>Al<sub>x</sub>B<sub>2</sub> single crystals with  $x = 0.12$  and  $0.21$  were grown under high-pressure conditions [11, 12] and were characterized and patterned as in [11, 12]. Two sets of samples with clean, shiny surface were investigated for each Al concentration. For the resistance measurements, well-shaped single crystals with both sides flat were selected from numerous samples. The temperature and the angular dependences of the resistance were measured from 0 to 9 T by using the AC transport option in a PPMS Quantum Design system.

Figure 1 shows the resistivity  $\rho$  of the Mg<sub>1-x</sub>Al<sub>x</sub>B<sub>2</sub> single crystals ( $x = 0, 0.12$ , and  $0.21$ ) as a function of temperature. As the Al concentration increases,  $T_c$  decreases. The  $T_c$ 's are 30.8 K and 25.5 K for  $x = 0.12$  and  $x = 0.21$ , respectively. The data for  $x = 0$  were taken from Ref. [4] and  $T_c$  of this sample was around 37 K. Previously, for MgB<sub>2</sub> single crystals, the resistance was reported to follow the Bloch-Grüneisen (BG) formula with a Debye temperature of  $\Theta_D \sim 1100$  K [11]. This implied that the normal-state transport properties were well described by an electron-phonon interaction without considering an electron-electron interaction. To check whether this is the case in Al-doped single crystals, we fitted the  $\rho(T)$  data with the BG formula, where fitting parameters are  $\Theta_D$  and residual resistivity  $\rho_0$ . The solid lines in the figure are the BG theoretical curves and describes the  $\rho(T)$  data well. The value of  $\Theta_D$  in Al-doped single crystals is  $\sim 1000$  K, which is similar to that of MgB<sub>2</sub> single crystals.  $\rho_0$  increases monotonically with doping, and the fitted values of  $\rho_0$  are 1.63, 21.4, and 32.2  $\mu\Omega$  cm for  $x = 0.0, 0.12$ , and  $0.21$ , respectively. The inset of Fig. 1 shows the normalized low-field magnetization for zero-field-cooled state of

$\text{Mg}_{1-x}\text{Al}_x\text{B}_2$  single crystals extracted from the same batch of single crystals as was used for the resistivity measurements. The  $T_c$ 's determined from the resistivity and from the low-field magnetization were virtually the same.

Figure 2 (a) and (b) show, as an example, the temperature dependences of the resistances of the  $x = 0.12$  sample for  $H \parallel c$  and  $\parallel ab$ , respectively. As with  $\text{MgB}_2$  single crystals, this sample shows surface superconductivity: As the temperature decreases, the resistance first decreases linearly and then suddenly drops to zero. In the region of linear decrease, the resistance depends on the applied current, and a higher current induces a higher resistance. The drop in the resistance indicates the onset of bulk superconductivity. Particularly at high currents ( $I = 3$  mA) for  $H \parallel c$ , a peak, which is absent at low currents ( $I = 1$  mA), appears. The current dependence of this peak suggests that it is due to the peak effect, observed in  $\text{MgB}_2$  single crystals [13]. The upper critical fields can be determined unambiguously as the points where the resistance drops to zero in the curves for  $I = 1$  mA. Those points are indicated by the arrows.

In Fig. 3(a),  $H_{c2}^c(T)$  and  $H_{c2}^{ab}(T)$  for  $x = 0.12$  and  $0.21$  are plotted, where  $H_{c2}^c(T)$  and  $H_{c2}^{ab}(T)$  are  $H_{c2}(T)$ 's for  $H \parallel c$  and for  $H \parallel ab$ , respectively. For comparison, we also insert  $H_{c2}(T)$  for  $x = 0.0$ , which was taken from Ref. [4]. Interestingly, both  $H_{c2}^c(T)$  and  $H_{c2}^{ab}(T)$  decrease with increasing Al doping. As a result, the extrapolated  $H_{c2}^c(0)$  and  $H_{c2}^{ab}(0)$  are reduced. While the decrease in  $H_{c2}^{ab}(0)$  is consistent with the results for polycrystalline samples, the decrease in  $H_{c2}^c(0)$  is not. In a study by Angst *et al.*, a small increase in  $H_{c2}^c(0)$  was observed at an Al doping of 10 % [14]. By comparing  $H_{c2}(0)$  in both Al- and C-doped  $\text{MgB}_2$ , they concluded that in Al-doped samples, the shift in the Fermi level was dominant in determining  $H_{c2}(T)$  while in C-doped samples, disorder played a major role. However, in light of the huge increase in  $\rho_0$ , the effects of disorder are not negligible and should be taken into account. Another clue to the degree of dirtiness in  $\text{Mg}_{1-x}\text{Al}_x\text{B}_2$  single crystals for  $x = 0.12$  and  $x = 0.21$  can be found in the shape of  $H_{c2}^c(T)$  near  $T_c$ . While  $\text{MgB}_2$  single crystals show a linear decrease in  $H_{c2}^c(T)$  near  $T_c$ , close inspection reveals that an upward curvature gradually appears with Al doping. This becomes even clearer if  $H_{c2}^c(T)$  for  $x = 0$  is compared with that for  $x = 0.21$ . The upward curvature is consistent with the two-gap dirty-limit theory.

Since the variations in  $H_{c2}(T)$  with Al doping appear to agree well with the two-gap theory, we quantitatively analyzed our  $H_{c2}(T)$  data by using the dirty-limit theory [6, 7].

For  $x = 0$ , the dirty limit model may be inappropriate because pure MgB<sub>2</sub> crystals are considered to be in the clean limit [15]. If interband impurity scattering is assumed to be zero,  $H_{c2}(T)$  for  $H \parallel c$  is given by

$$a_0 [\ln t + U(h)] [\ln t + U(\eta h)] + a_2 [\ln t + U(\eta h)] + a_1 [\ln t + U(h)] = 0, \quad (1)$$

where  $t = T/T_c$ ,  $U(x) = \Psi(1/2 + x) - \Psi(x)$ ,  $\Psi(x)$  is the Euler digamma function,  $h = H_{c2}D_{\sigma}^{ab}/2\phi_0T$ ,  $\phi_0$  is the magnetic flux quantum,  $\eta = D_{\pi}^{ab}/D_{\sigma}^{ab}$ ,  $D_{\sigma,\pi}^{ab}$  is the in-plane electron diffusivity of the  $\sigma$  and the  $\pi$  bands, and  $a_{0,1,2}$  are constants derived from the electron-phonon coupling constants ( $\lambda_{mn}^{ep}$ ) and the Coulomb pseudopotentials ( $\mu_{mn}$ ). The precise definitions of  $a_{0,1,2}$  can be found in Ref. 6. For  $H \parallel ab$ , the in-plane diffusivities in Eq. 1 can be replaced by  $[D_{\sigma,\pi}^{ab}D_{\sigma,\pi}^c]^{1/2}$ , where  $D_{\sigma,\pi}^c$  are the out-of-plane electron diffusivities of the  $\sigma$  and the  $\pi$  bands, respectively. Equation 1 can be generalized to the anisotropic case of an inclined field by replacing the diffusivities with the angle-dependent diffusivities  $D_{\sigma}(\theta)$  and  $D_{\pi}(\theta)$  for both bands, where  $D_{\sigma,\pi}(\theta) = [(D_{\sigma,\pi}^{ab})^2 \cos^2 \theta + D_{\sigma,\pi}^{ab}D_{\sigma,\pi}^c \sin^2 \theta]^{1/2}$ . For the four input parameters  $\lambda_{mn} = \lambda_{mn}^{ep} - \mu_{mn}$  at each Al doping level, which reflects the change in the electronic structure by electron doping, we used the values determined from first-principle calculations [16], and we obtained the numerical value of the diffusivity for each band.

In our samples, the interband impurity scattering is believed not to be significant or, if any, to be negligible to the first approximation. This is because the interband impurity scattering was predicted to eliminate the distinction of each superconducting gap, destructing two-gap features [17]. Therefore, the upward curvature, which is the hallmark of the two-gap superconductivity would have not been observed, if interband impurity scattering were significant.

The solid lines in Fig. 3(a) present the theoretical two-gap dirty-limit curves of  $H_{c2}(T)$  for  $x = 0.12$  and  $0.21$ . The optimized values of  $D_{\sigma}^{ab,c}$ ,  $D_{\pi}^{ab,c}$ , and  $H_{c2}^{ab,c}(0)$  from the fits are summarized in Table I. The upward curvature observed near  $T_c$  for  $x = 0.12$  and  $0.21$ , which is typical when  $\sigma$  bands are dirtier than  $\pi$  bands [6], may indicate dirtier  $\sigma$  bands. If the  $\pi$  bands are dirtier than the  $\sigma$  bands, the upward curvature near  $T_c$  should disappear; instead, a huge increase in  $H_{c2}(T)$  should appear at low temperatures. The dashed line for  $x = 0$  is a guide to eyes.

Quantitatively, the values of  $D_{\sigma}^{ab,c}$  and  $D_{\pi}^{ab,c}$  really prove dirty  $\sigma$  bands ( $D_{\sigma}^{ab,c} \ll D_{\pi}^{ab,c}$ ),

which is consistent with the shape of  $H_{c2}(T)$ . Dirty  $\sigma$  bands were also observed in Al-doped  $\text{MgB}_2$  polycrystalline samples [18]. The electron diffusivity along the  $c$  direction in the  $\pi$  bands is noted to decrease with Al doping while that in the  $ab$  plane virtually does not change. This originates from pronounced impurity scattering in the  $\pi$  bands as the Al concentration is increased. The pronounced impurity scattering, however, is not isotropic as is normally assumed. Along the  $c$  direction, impurity scattering is more enhanced than in the  $ab$  plane. Similarly, Al doping influences impurity scattering in the  $\sigma$  bands. In this case, the electron diffusivity along the  $c$  direction increases with Al doping while that in  $ab$  plane virtually is unchanged. Consequently, the  $\sigma$  bands become more isotropic, which is reflected in the ratio  $D_\sigma^{ab}/D_\pi^c$  and this value decreases as Al content increases. The isotropization of the  $\sigma$  bands is believed to be due to not only the anisotropic impurity scattering but also the change in the electronic structure that Al doping induces.

The same set of electron diffusivities as in Table I can explain  $H_{c2}(\theta)$  for  $x = 0.12$  and  $0.21$ , as shown in Fig. 3(b). The solid lines indicate the theoretical curves calculated from the dirty-limit two-gap theory. The dotted lines are the theoretical curves of the one-gap GL model. The error bars in this data are comparable to or less than the symbol size. The two-gap theory describes the data better than the GL model for  $x = 0.12$ . For  $x = 0.12$ , a small difference between the two-gap theory and the GL model is apparent and as predicted, is most pronounced at the middle-angle regions. This is a strong indication of the two-gap nature of Al-doped  $\text{MgB}_2$  single crystals. This behavior is very similar to that of  $\text{MgB}_2$  single crystals, where a deviation from GL behavior was observed to be peaked at  $T \approx 0.8T_c$ . For  $x = 0.21$ , the difference between the two-gap theory and the anisotropic GL model is very tiny, as is the case for the temperatures we investigated. Despite the indistinction between the anisotropic GL model and the two-gap theory for this doping, the shapes of the  $H_{c2}(T)$  curves and the values of the fitted diffusivities guarantee the existence of two distinct gaps. If the sample for  $x = 0.21$  followed the one-gap GL model, the upward curvature would not be observed.

Finally,  $\gamma_H(T)$  for  $x = 0, 0.12$ , and  $0.21$ , extracted from the  $H_{c2}(T, \theta)$  data, are plotted as functions of the reduced temperature  $T/T_c$  in the inset of Fig. 3(a). The values of  $\gamma_H$  are systematically reduced, and for  $x = 0.21$ ,  $\gamma_H$  is virtually temperature-independent at high temperatures, slightly increasing at low temperatures. The  $\gamma_H$  at low temperatures significantly changes with Al doping and the  $\gamma_H$ 's merge to  $2 - 2.5$  at  $T = T_c$  for all doping

levels. This behavior is thought to result from the isotropization of the  $\sigma$  bands. The decreasing tendency of  $\gamma_H$  with increasing temperature for  $x = 0.12$  and  $0.21$  is in good agreement with the case of dirty  $\sigma$  bands, predicted by using the dirty-limit two-gap theory.

If the effects of impurity scattering can be ignored in  $x = 0.12$  and  $0.21$  single crystals,  $H_{c2}$  will evolve according to changes in the electronic structure and in the lattice constant. Among these, the main effect is due to changes in the electronic structure caused by doping with electrons, resulting in a shift of Fermi level  $E_F$  to higher energies. At moderate doping levels, where a rigid band model is valid, an increase in  $E_F$  modifies the band-averaged Fermi velocities, primarily in the  $\sigma$  bands and the  $\gamma_H(0)$ , which is  $\gamma_{v_F} \equiv v_{F,\sigma}^{ab}/v_{F,\sigma}^c$  in the clean limit. Here,  $v_{F,\sigma}^{ab(c)}$  is the in-plane (out-of-plane) Fermi velocity of the  $\sigma$  bands. According to the calculation by Putti *et al.* [19],  $v_{F,\sigma}^c$  remains approximately constant while  $v_{F,\sigma}^{ab}$  substantially decreases with Al doping for  $x < 0.3$ . At doping levels of  $x = 0.0, 0.12$ , and  $0.21$ , that calculation produced  $\gamma_{v_F} = 5.6, 5$ , and  $4.2$ , respectively. The value at  $x = 0.0$  is nearly consistent with  $\gamma_H(0)$  estimated from the experimental data, as shown in the inset of Fig. 3(a). In contrast, the values at  $x = 0.12$  and  $0.21$  are significantly larger than the estimated  $\gamma_H(0)$ . In fact, the  $\gamma_H(0)$ 's at  $x = 0.12$  and  $0.21$  are better represented by the parameter  $\gamma_\sigma \equiv \sqrt{D_\sigma^{ab}/D_\sigma^c}$ , which contains information on not only the Fermi velocity but also impurity scattering. Therefore, as we said before,  $\text{Mg}_{1-x}\text{Al}_x\text{B}_2$  single crystals ( $x = 0.12$  and  $0.21$ ) are in the dirty limit with anisotropic impurity scattering. This is in sharp contrast to the conclusions for Al-doped  $\text{MgB}_2$  polycrystalline samples [14, 19]. Those polycrystalline samples might have less impurities than single crystals, which is very improbable in normal situations. It is noted that while  $\gamma_\sigma$  decreases with Al doping,  $\gamma_\pi$  increases from 1.1 to 1.8

In fact, the electron diffusivities are related to the value of resistivity by the relation of  $1/\rho \propto N_\sigma D_\sigma + N_\pi D_\pi$  [6], where  $N_\sigma$  and  $N_\pi$  are partial densities of state in  $\sigma$  and  $\pi$  bands, respectively. In the present case, since the electron diffusivities in the  $\pi$  bands are larger than those in the  $\sigma$  bands, the electron diffusivities in the  $\pi$  bands determine the resistivities of our samples and resistivity should increase with  $x$ . This tendency holds in our samples. We calculated the values of resistivities by using the obtained diffusivity values and the partial densities of state calculated by Ummarino *et al.* [16] and obtained 10 and 12  $\mu\Omega\text{cm}$  for  $x = 0.12$  and  $x = 0.21$ , respectively. The discrepancy of the absolute values, especially for  $x = 0.21$  might originate from a large error in calculating the resistivity of small-sized samples.

To summarize, we investigated the effect of Al substitution on  $H_{c2}(T, \theta)$  of MgB<sub>2</sub> single crystals. From an analysis of  $H_{c2}(T, \theta)$  within the dirty-limit two-gap theory, we found that Al substitution influenced the electronic structure complexly; in the  $\pi$  bands, it increased impurity scattering along the  $c$  direction while it made the  $\sigma$  bands less anisotropic. Accordingly,  $\gamma_H(T)$  was systematically decreased and for  $x = 0.21$ ,  $\gamma_H$  was virtually temperature-independent. The isotropization, especially of the  $\sigma$  bands, originates not only from increased anisotropic impurity scattering but also from electron doping. In  $H_{c2}(\theta)$ , we also observed a strong indication of the dirty-limit two-gap nature of Al-doped MgB<sub>2</sub>.

### Acknowledgments

This work is supported by the Ministry of Science and Technology of Korea through the Creative Research Initiative Program and by the Asia Pacific Center for Theoretical Physics. This work was partially supported by the National Research Laboratory Program through the Korea Institute of Science and Technology Evaluation and Planning.

<sup>†</sup>present address : Department of Physics, Chungbuk National University, Cheongju 361-763, Republic of Korea

- 
- [1] Amy Y. Liu, I. I. Mazin, and Jens Kortus, Phys. Rev. Lett. **87**, 087005 (2001).
  - [2] Hyoung Joon Choi, David Roundy, Hong Sun, Marvin L. Cohen, Steven G. Louie, Nature **418**, 758 (2002).
  - [3] S. Souma, Y. Machida, T. Sato, T. Takahashi, H. Matsui, S.-C. Wang, H. Ding, A. Kaminski, J. C. Campuzano, S. Sasaki, K. Kadowaki, Nature **423**, 65 (2003).
  - [4] L. Lyard, P. Samuely, P. Szabo, T. Klein, C. Marcenat, L. Paulius, K. H. P. Kim, C. U. Jung, H.-S. Lee, B. Kang, S. Choi, S.-I. Lee, J. Marcus, S. Blanchard, A. G. M. Jansen, U. Welp, G. Karapetrov, and W. K. Kwok, Phys. Rev. B **66**, 180502(R) (2002).
  - [5] T. Dahm and N. Schopohl, Phys. Rev. Lett. **91**, 017001 (2003).
  - [6] A. Gurevich, Phys. Rev. B **67**, 184515 (2003).
  - [7] A. A. Golubov and A. E. Koshelev, Phys. Rev. B **68**, 104503 (2003).

- [8] L. Lyard, P. Szabo, T. Klein, J. Marcus, C. Marcenat, K. H. Kim, B. W. Kang, H. S. Lee, and S. I. Lee, *Phys. Rev. Lett.* **92**, 057001 (2004).
- [9] Heon-Jung Kim, Byeongwon Kang, Min-Seok Park, Kyung-Hee Kim, Hyun Sook Lee, and Sung-Ik Lee, *Phys. Rev. B* **69**, 184514 (2004).
- [10] A. Rydh, U. Welp, A. E. Koshelev, W. K. Kwok, G. W. Crabtree, R. Brusetti, L. Lyard, T. Klein, C. Marcenat, B. Kang, K. H. Kim, K. H. P. Kim, H.-S. Lee, and S.-I. Lee, *Phys. Rev. B* **70**, 132503 (2004).
- [11] Kijoon H. P. Kim, Jae-Hyuk Choi, C. U. Jung, P. Chowdhury, Hyun-Sook Lee, Min-Seok Park, Heon-Jung Kim, J. Y. Kim, Zhonglian Du, Eun-Mi Choi, Mun-Seog Kim, W. N. Kang, Sung-Ik Lee, Gun Yong Sung, and Jeong Yong Lee, *Phys. Rev. B* **65**, 100510(R) (2002).
- [12] Byeongwon Kang, Heon-Jung Kim, Min-Seok Park, Kyung-Hee Kim, and Sung-Ik Lee, *Phys. Rev. B* **69**, 144514 (2004).
- [13] U. Welp, A. Rydh, G. Karapetrov, W. K. Kwok, G. W. Crabtree, Ch. Marcenat, L. Paulius, T. Klein, J. Marcus, K. H. P. Kim, C. U. Jung, H.-S. Lee, B. Kang, and S.-I. Lee, *Phys. Rev. B* **67**, 012505 (2003).
- [14] M. Angst, S. L. Bud'ko, R. H. T. Wilke, and P. C. Canfield, *Phys. Rev. B* **71**, 144512 (2005).
- [15] E. A. Yelland, J. R. Cooper, A. Carrington, N. E. Hussey, P. J. Meeson, S. Lee, A. Yamamoto, and S. Tajima, *Phys. Rev. Lett.* **88**, 217002 (2002).
- [16] G. A. Ummarino, R. S. Gonnelli, S. Massidda and A. Bianconi, *Physica C* **407**, 121 (2004).
- [17] A. A. Golubov and I. I. Mazin, *Phys. Rev. B* **55**, 15146 (1997).
- [18] Min-Seok Park, Heon-Jung Kim, Byeongwon Kang and Sung-Ik Lee, *Supercond. Sci. Technol.* **18**, 183 (2005).
- [19] M. Putti, C. Ferdeghini, M. Monni, I. Pallecchi, C. Tarantini, P. Manfrinetti, A. Palenzona, D. Daghero, R. S. Gonnelli, and V. A. Stepanov, *Phys. Rev. B* **71**, 144505 (2005).

TABLE I: Al content  $x$ , upper critical fields  $H_{c2}^{ab(c)}(0)$ , electron diffusivities along the  $ab$  plane (the  $c$  axis) in the  $\sigma$  and the  $\pi$  bands,  $D_{\sigma}^{ab(c)}$  and  $D_{\pi}^{ab(c)}$ , obtained by fitting the  $H_{c2}(T)$  data to the dirty-limit model.

$x$	$H_{c2}^{ab}(0)$ (T)	$H_{c2}^c(0)$ (T)	$D_{\sigma}^{ab}$ ( $m^2s^{-1}$ )	$D_{\sigma}^c$ ( $m^2s^{-1}$ )	$D_{\pi}^{ab}$ ( $m^2s^{-1}$ )	$D_{\pi}^c$ ( $m^2s^{-1}$ )
0.12	9.3	2.7	$7.6 \times 10^{-4}$	$5.9 \times 10^{-5}$	$3.7 \times 10^{-3}$	$3.0 \times 10^{-3}$
0.21	5.6	2.3	$6.0 \times 10^{-4}$	$1.0 \times 10^{-4}$	$4.8 \times 10^{-3}$	$1.4 \times 10^{-3}$

FIG. 1: Temperature dependence of the resistivity for  $Mg_{1-x}Al_xB_2$  single crystals ( $x = 0.0, 0.12,$  and  $0.21$ ). The solid lines are theoretical curves of the BG formula. The inset shows the normalized low-field magnetization in the zero-field-cooled state.

FIG. 3: (a) Temperature dependence of  $H_{c2}$  for  $Mg_{1-x}Al_xB_2$  single crystals ( $x = 0.0, 0.12,$  and  $0.21$ ). Open symbols represent  $H_{c2}(T)$  for  $H \parallel c$  and closed symbols represent  $H_{c2}(T)$  for  $H \parallel ab$ . The data for  $x = 0.0$  were taken from Ref. [4]. The inset shows temperature dependence of  $\gamma_H$ . The open triangle is  $\gamma_{v_F} \equiv v_{F,\sigma}^{ab}/v_{F,\sigma}^c$ , and the open circle and square are  $\gamma_{\sigma} \equiv \sqrt{D_{\sigma}^{ab}/D_{\sigma}^c}$ 's. (b) Angular dependence of  $H_{c2}$ . The solid lines are the theoretical curves for the dirty-limit two-gap model, and the dotted lines are those for the Ginzburg-Landau theory.

FIG. 2: Temperature dependence of the resistance for (a)  $H \parallel c$  and (b)  $H \parallel ab$ .

Figure 1 by Kim *et al.*

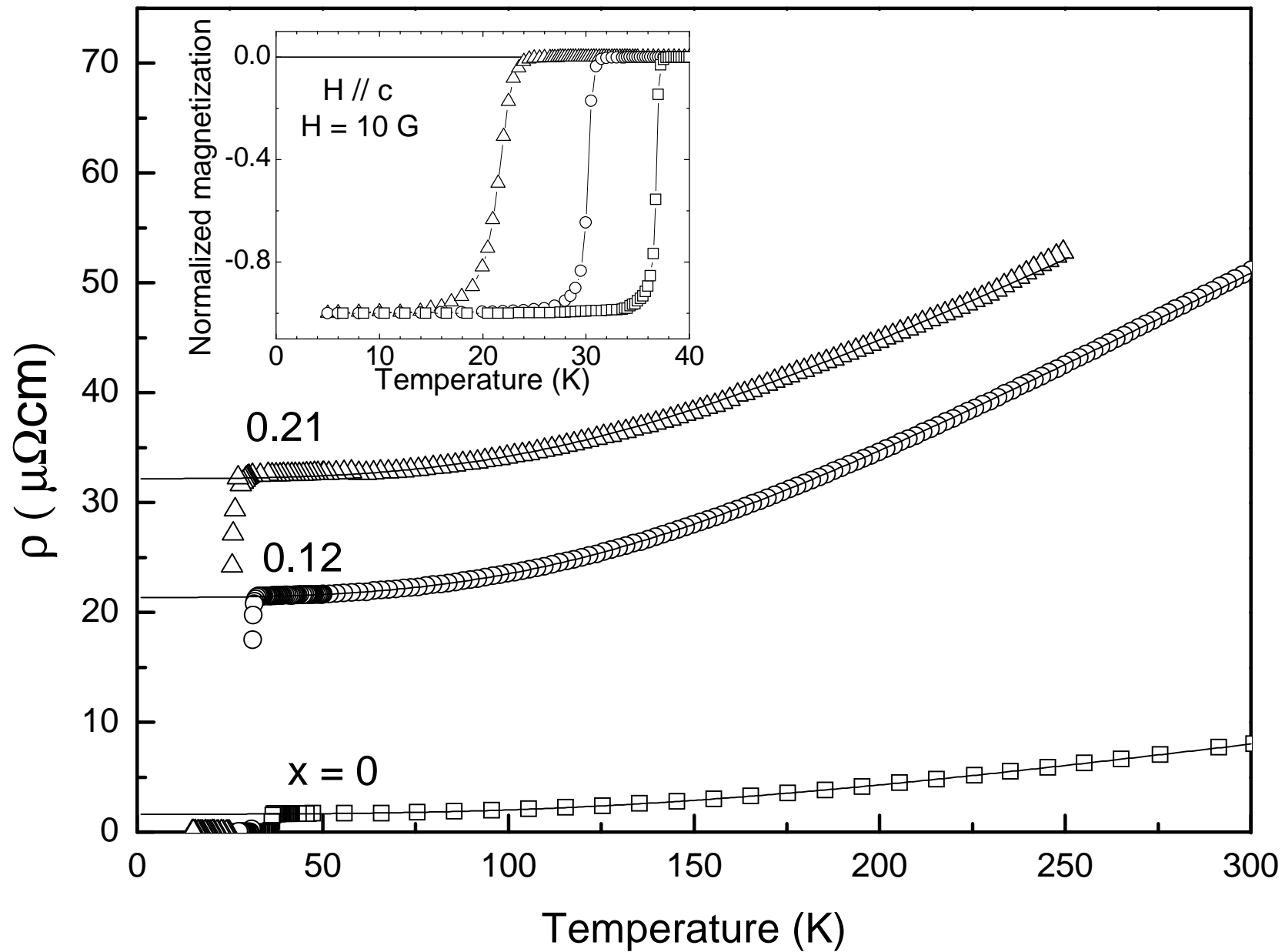


Figure 2 by Kim *et al.*

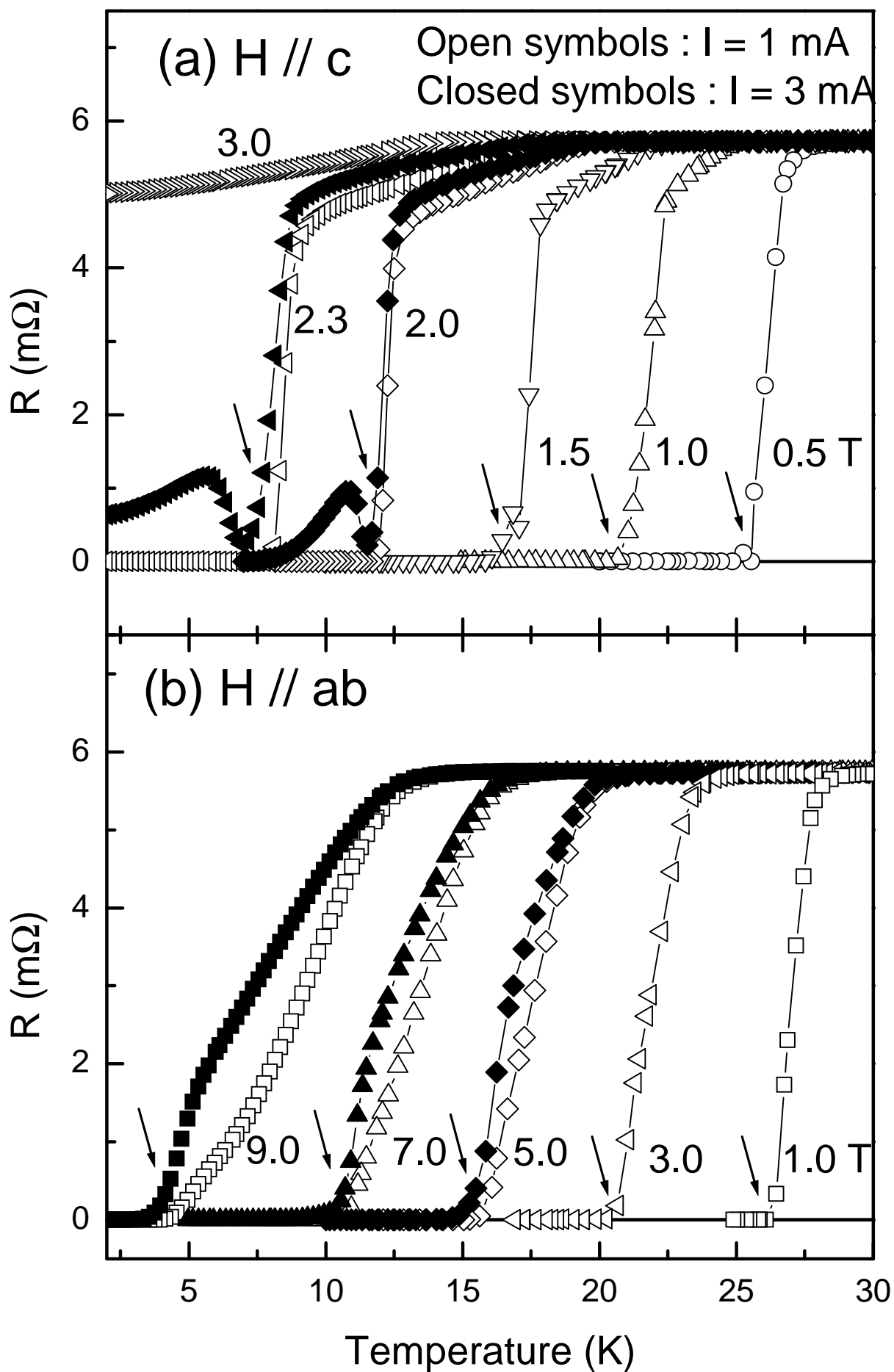


Figure 3(a) by Kim *et al.*

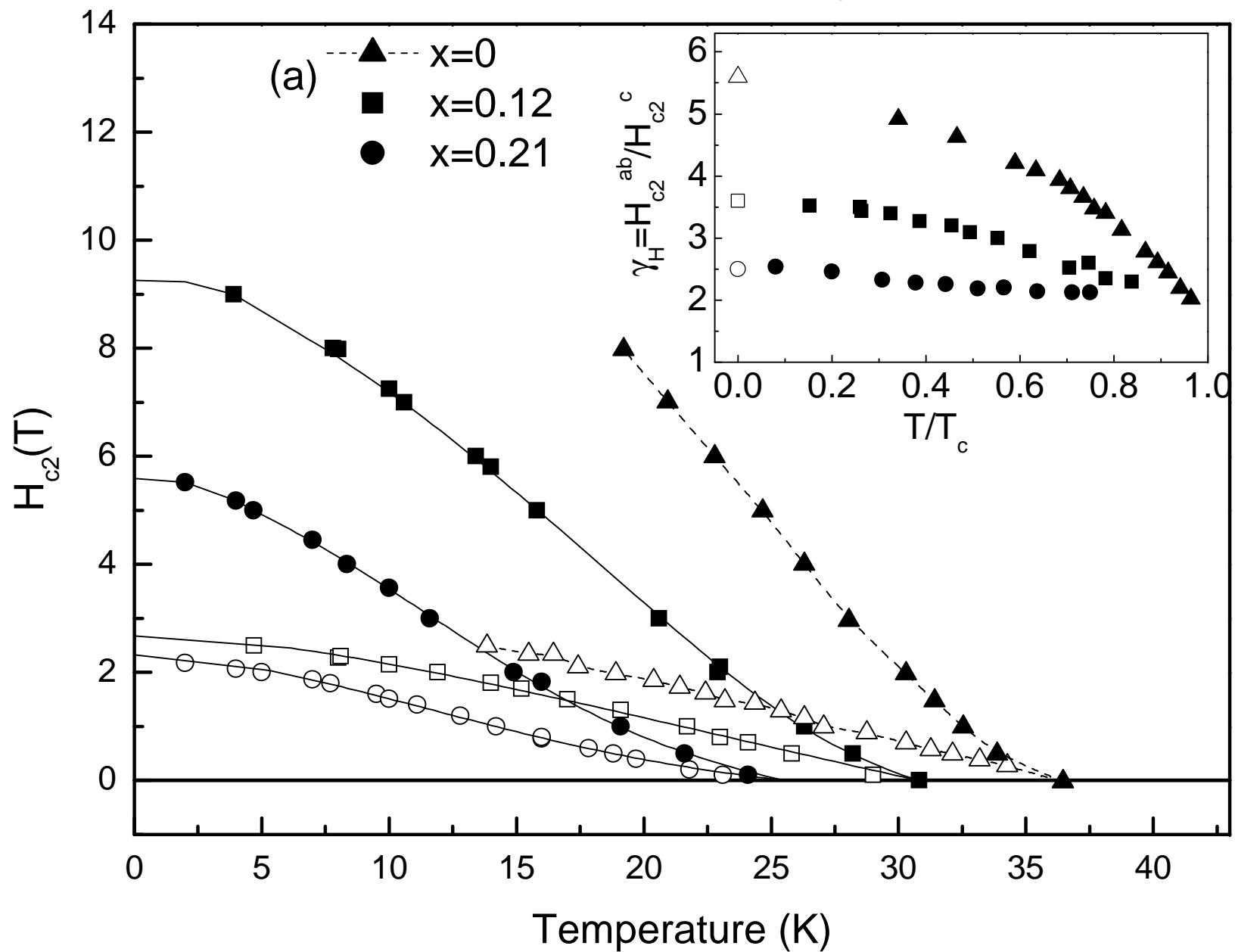


Figure 3(b) by Kim *et al.*

